ChemPubSoc Europe

DOI: 10.1002/open.201600158

Open Access ChemistryOPEN Communications

Targeted Fluoro Positioning for the Discovery of a Potent and Highly Selective Matrix Metalloproteinase Inhibitor

Thomas Fischer and Rainer Riedl*[a]

In memory of Margrit Stark-Siebold and Wolfgang Hampe

The incorporation of fluorine atoms into functional molecules is of wide interest in synthetic organic chemistry as well as cognate disciplines. In particular, in medicinal chemistry, there is a strong desire to positively influence the physicochemical molecular properties of drug compounds by introducing fluorine into biologically active molecules. Here, we present targeted fluoro positioning as the key design principle of converting a weak matrix metalloproteinase-13 (MMP-13) inhibitor into a very potent (IC_{50} = 6 nM) and highly selective (selectivity factors of > 1000 over MMP-1, 2, 3, 7, 8, 9, 10, 12, 14) inhibitor with excellent plasma and microsomal stability, and no binding to the hERG channel (hERG: human ether-a-go-go related gene).

Fluorine-containing compounds have gained emerging interest in chemistry, as synthetic strategies have evolved to allow the diverse use of this formerly exotic element.[1–6] Owing to its small size, with a van der Waals radius of 1.47 Å (in comparison to 1.20 Å for hydrogen and 1.52 Å for oxygen), and its high electronegativity (3.98 according to the Pauling scale in contrast to 2.20 for hydrogen), fluorine can be incorporated into molecules to substitute a hydrogen atom and to alter the physicochemical properties without applying major changes to the size of the compound.[7,8] The introduction of fluorine atoms to drug molecules can modulate a broad range of drug properties. Amongst others, it is reported to have an effect on the pharmacokinetic profile, membrane permeability, and the conformation of a molecule.[9–12] Deployment of fluorine in identified enzyme inhibitors is of great significance in the development process from initial hits to lead compounds when attention is paid to preclinical properties.[13–16]

Matrix metalloproteinase-13 (MMP-13) is, within its superfamily of zinc-dependent endopeptidases, the most efficient member with respect to the degeneration of type II collagen and is, therefore, an established target for the treatment of diseases in which tissue remodeling is out of balance, such as in osteoarthritis and a variety of cancers.[17–21] Early inhibitors of the target class incorporated strong metal chelators such as hydroxamic acids. These broad-band inhibitors were highly potent, but did not display satisfying selectivity, whereby clinical trials failed because of joint-stiffening and painful side effects like musculoskeletal syndrome (MSS).[22,23] Later developments led to allosteric binders, occupying the selectivity loop within the S_1' pocket, sparing the interaction to the zinc ion.[24–26] Equipping selective allosteric inhibitors with weaker metal-chelating groups, such as carboxylic acid for example, can improve the potency of the inhibitors while maintaining the selectivity profile.[27–29]

We selected MMP-13 as the target protein for our structure-based drug design, employing water-mediated interactions by targeted fluoro positioning for the optimization of potency, selectivity, and preclinical ADME properties. Recently, we identified phthalimide derivative **1** (Figure 1) as a weak allosteric inhibitor of MMP-13, displaying an IC_{50} value of 9.8 μM and a rather poor stability profile in liver microsomes and plasma.[30]

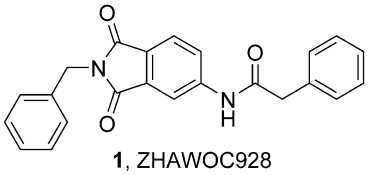

1, ZHAWOC928

Figure 1. Previously identified weak MMP-13 inhibitor **1** displaying poor stability in plasma and liver microsomes.

Starting with the initial weak inhibitor **1**, we applied structure-based design to attach a zinc-binding moiety to the phthalimide scaffold to gain a higher binding affinity. According to our modeling studies, derivatives of **1** modified by the attachment of carboxylic acids through growing methylene linkers can bind to the allosteric binding site as well as to the catalytic zinc ion (Figure 2).[28]

We found that the *para*-substituted derivatives with chain lengths between 2 and 5 carbon atoms are reasonable for the elevation of inhibitor potency. Previous work indicated that a chain length of 4 carbon atoms between the phenolic oxygen and the zinc-recognizing carboxylic acid is the most promising member within this set of compounds.[27] Subse-

[a] *T. Fischer, Prof. Dr. R. Riedl*
Institute of Chemistry and Biotechnology
Center for Organic and Medicinal Chemistry
Zurich University of Applied Sciences (ZHAW)
Einsiedlerstrasse 31, 8820 Wädenswil (Switzerland)
E-mail: rainer.riedl@zhaw.ch

Supporting information and the ORCID identification number(s) for the author(s) of this article can be found under http://dx.doi.org/10.1002/open.201600158.

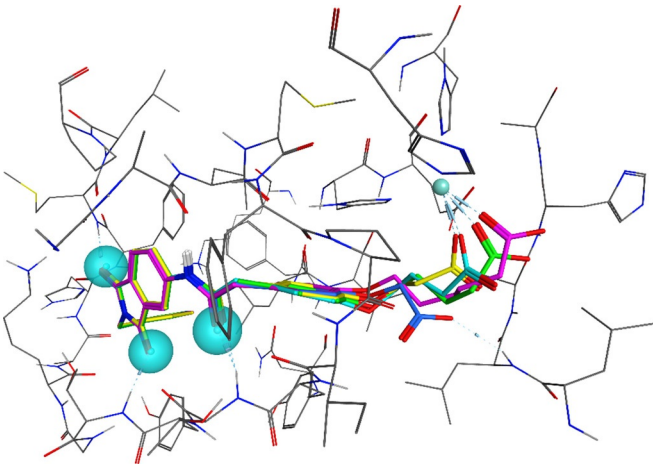

Figure 2. Molecular modeling of inhibitor **1** and its elongated derivatives in PDB 2OW9:[25] pharmacophore displayed in cyan spheres; different lengths of methylene linkers depicted in blue [CH_2], yellow [$(CH_2)_2$], cyan [$(CH_2)_3$], green [$(CH_2)_4$], magenta [$(CH_2)_5$].

quently, we investigated the possibility to probe water-mediated interactions through targeted fluoro positioning in the S_1' pocket (Figure 3). Although the *meta* position as well as the *para* position indicated water-mediated interactions by the fluoro atom within comparable distances (2.5 Å for *meta* substitution and 2.7 Å for *para* substitution), no possible interaction for *ortho* substitution could be detected (Figure 3 and the Supporting Information).

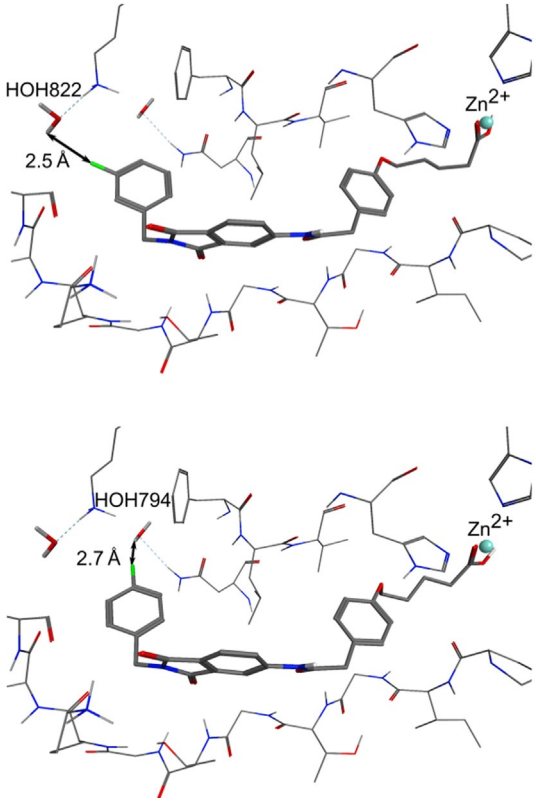

Figure 3. Targeted fluoro positioning to probe water-mediated interactions.

As displayed in Figure 3, owing to the small van der Waals radius of fluorine, we could omit sterically demanding alterations in this region of the receptor. This is beneficial because of the rather limited space in the S_1' pocket. The *para*-fluorinated compound was of highest interest to us, as it does not display a hydrogen atom in the *para* position, which is prone to metabolic degradation by cytochrome P450 enzymes.[31–34] Driven by the promising results derived from the molecular design approach, we synthesized compounds **2a–g** (Figure 4) in order to test our hypotheses with biological inhibitory data (Table 1). The synthetic route and all experimental details are given in the Supporting Information.

All synthesized compounds exhibited a higher potency compared to inhibitor **1**. Carboxylic acid **2c** showed the lowest IC_{50} value of the non-fluorinated compounds (35 nM), validating our structure-based design with a chain length of 4 carbon atoms for the optimal linker.

Equipping this molecule with a fluorine atom in the *para* position resulted in compound **2d**, which displayed the highest affinity (IC_{50} = 6 nM) of all tested molecules with a very high ligand efficiency and lipophilic ligand efficiency. An alteration of the fluorine atom to the *meta* position was tolerated with

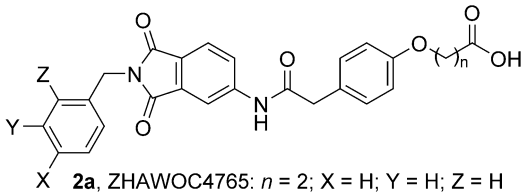

2a, ZHAWOC4765: *n* = 2; X = H; Y = H; Z = H
2b, ZHAWOC4766: *n* = 3; X = H; Y = H; Z = H
2c, ZHAWOC5131: *n* = 4; X = H; Y = H; Z = H
2d, ZHAWOC5684: *n* = 4; X = F; Y = H; Z = H
2e, ZHAWOC6023: *n* = 4; X = H; Y = F; Z = H
2f, ZHAWOC6024: *n* = 4; X = H; Y = H; Z = F
2g, ZAHWOC5133: *n* = 5; X = H; Y = H; Z = H

Figure 4. Synthesized fluoro probes **2d–f** for the targeted inhibition of MMP-13 and non-fluorinated compounds **2a–c** and **2g**.

Table 1. MMP-13 inhibitory data for compounds **1** and **2a–g**.

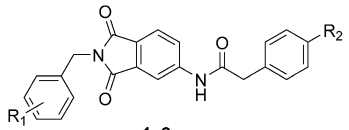

1, 2a-g

Inhibitor	R1	R2	IC_{50} [nM]	clog*P*	*LE*[a]	*LLE*[b]
1	H	H	9800 ± 3400	3.94	0.25	1.07
2a	H	$O(CH_2)_2COOH$	2244 ± 200	3.21	0.23	2.44
2b	H	$O(CH_2)_3COOH$	556 ± 125	3.56	0.25	2.69
2c	H	$O(CH_2)_4COOH$	35 ± 0.6	4.00	0.29	3.46
2d	4-F	$O(CH_2)_4COOH$	6 ± 2.5	4.15	0.31	4.07
2e	3-F	$O(CH_2)_4COOH$	10 ± 1.6	4.15	0.30	3.85
2f	2-F	$O(CH_2)_4COOH$	134 ± 39	4.15	0.26	2.72
2g	H	$O(CH_2)_5COOH$	151 ± 31	4.45	0.26	2.37

[a] The ligand efficiency (*LE*) was calculated as $1.4(-\log IC_{50})/N$, where *N* equals the number of non-hydrogen atoms. [b] The lipophilic ligand efficiency (*LLE*) was calculated as $(-\log IC_{50})-\text{clog}P$.

comparable potency (IC_{50} = 10 nM) in accordance with our concept of targeting water-mediated interactions by the fluoro probe (Figure 3). The boost in potency from **2c** to **2d** and **2e** corresponds well with our hypothesis that directed fluorine incorporation in this region of the ligand will have a beneficial influence on the binding interaction between the enzyme and its inhibitor. The almost six-fold improvement in potency from **2c** to **2d** is in line with literature data for this type of interaction and supports our design strategy.[35,36]

For the two most potent fluorinated compounds, **2d** and **2e**, a selectivity profile was generated that compared the inhibition of MMP-13 with other members of this challenging target family. The fluorinated compounds showed outstanding selectivity factors of >1000 against MMP-1, 2, 3, 7, 8, 9, 10, 12, and 14. For the most potent inhibitor **2d**, as well as for the initial weak inhibitor **1**, in vitro ADME properties were determined. Shake-flask solubility at pH 7.4, mouse plasma and mouse microsomal stability, and hERG binding were measured (hERG: human ether-a-go-go related gene). Fluorinated inhibitor **2d** showed consistently superior characteristics compared to the initial inhibitor **1**. The microsomal stability improved dramatically from a half-life $T_{1/2}$ = 30 min and an intrinsic clearance Cl_{int} = 55 μL min^{-1} mg^{-1} (**1**) to $T_{1/2}$ > 240 min and Cl_{int} < 10 μL min^{-1} mg^{-1} (**2d**). In addition, the plasma stability could be enhanced from $T_{1/2}$ = 181 min (**1**) to >240 min (**2d**) and the solubility in phosphate-buffered saline pH 7.4 improved from 58 ± 3 μM (**1**) to 94 ± 2 μM (**2d**). Measurements of hERG inhibition of the novel inhibitor **2d** revealed no hERG-related liability for drug toxicity. The excellent pharmacokinetic profile in combination with the high potency and outstanding selectivity data qualify inhibitor **2d** for further studies in relevant disease models.

In conclusion, this study shows how probing the selectivity loop of MMP-13 with targeted fluoro positioning enhances the ligands potency and selectivity as well as its ADME properties. This approach can also be adopted for other target proteins. By using structure-based design to target the catalytic zinc ion by a carboxylic acid and water-mediated interactions through directed fluoro positioning in the selectivity loop, we could develop an initially weak inhibitor with a rather poor pharmacokinetic profile into a potent and highly selective inhibitor of MMP-13 with very high murine plasma and microsomal stability. Suitable solubility and the absence of hERG liability make this inhibitor a valuable candidate for studies in in vivo disease models for cancer, arthritis, or other indications where the selective inhibition of MMP-13 is of interest.

Acknowledgements

The authors are grateful to the Zurich University of Applied Sciences (ZHAW) for financial support. We thank Roland Josuran for HRMS measurements and Loris Peduto for technical assistance.

Conflict of Interest

The authors declare no conflict of interest.

Keywords: drug design · drug discovery · medicinal chemistry · metalloenzymes · structure–activity relationships

[1] C. N. Neumann, T. Ritter, *Angew. Chem. Int. Ed.* **2015**, *54*, 3216 – 3221; *Angew. Chem.* **2015**, *127*, 3261 – 3267.
[2] T. Liang, C. N. Neumann, T. Ritter, *Angew. Chem. Int. Ed.* **2013**, *52*, 8214 – 8264; *Angew. Chem.* **2013**, *125*, 8372 – 8423.
[3] T. Ahrens, J. Kohlmann, M. Ahrens, T. Braun, *Chem. Rev.* **2015**, *115*, 931 – 972.
[4] X. Yang, T. Wu, R. J. Phipps, F. D. Toste, *Chem. Rev.* **2015**, *115*, 826 – 870.
[5] K. Müller, C. Faeh, F. Diederich, *Science* **2007**, *317*, 1881 – 1886.
[6] A. Tlili, F. Toulgoat, T. Billard, *Angew. Chem. Int. Ed.* **2016**, *55*, 11726 – 11735; *Angew. Chem.* **2016**, *128*, 11900 – 11909.
[7] A. Bondi, *J. Phys. Chem.* **1964**, *68*, 441 – 451.
[8] L. Pauling, *The Nature of the Chemical Bond: An Introduction to Modern Structural Chemistry*, Cornell University Press, Ithaca, NY, **1960**.
[9] A. Di Capua, C. Sticozzi, S. Brogi, M. Brindisi, A. Cappelli, L. Sautebin, A. Rossi, S. Pace, C. Ghelardini, L. Di Cesare Mannelli, G. Valacchi, G. Giorgi, A. Giordani, G. Poce, M. Biava, M. Anzini, *Eur. J. Med. Chem.* **2016**, *109*, 99 – 106.
[10] A. D. Kerekes, S. J. Esposite, R. J. Doll, J. R. Tagat, T. Yu, Y. Xiao, Y. Zhang, D. B. Prelusky, S. Tevar, K. Gray, G. A. Terracina, S. Lee, J. Jones, M. Liu, A. D. Basso, E. B. Smith, *J. Med. Chem.* **2011**, *54*, 201 – 210.
[11] S. Yamazaki, Z. Shen, Y. Jiang, B. J. Smith, P. Vicini, *Drug Metab. Dispos.* **2013**, *41*, 1285 – 1294.
[12] M. Pettersson, X. Hou, M. Kuhn, T. T. Wager, G. W. Kauffman, P. R. Verhoest, *J. Med. Chem.* **2016**, *59*, 5284 – 5296.
[13] E. P. Gillis, K. J. Eastman, M. D. Hill, D. J. Donnelly, N. A. Meanwell, *J. Med. Chem.* **2015**, *58*, 8315 – 8359.
[14] S. Purser, P. R. Moore, S. Swallow, V. Gouverneur, *Chem. Soc. Rev.* **2008**, *37*, 320 – 330.
[15] H.-J. Böhm, D. Banner, S. Bendels, M. Kansy, B. Kuhn, K. Müller, U. Obst-Sander, M. Stahl, *ChemBioChem* **2004**, *5*, 637 – 643.
[16] M. F. Chellat, L. Raguž, R. Riedl, *Angew. Chem. Int. Ed.* **2016**, *55*, 6600 – 6626; *Angew. Chem.* **2016**, *128*, 6710 – 6738.
[17] H. Nagase, J. F. Woessner, *J. Biol. Chem.* **1999**, *274*, 21491 – 21494.
[18] I. Bertini, V. Calderone, M. Fragai, C. Luchinat, M. Maletta, K. J. Yeo, *Angew. Chem. Int. Ed.* **2006**, *45*, 7952 – 7955; *Angew. Chem.* **2006**, *118*, 8120 – 8123.
[19] T. E. Cawston, A. J. Wilson, *Best Pract. Res. Clin. Rheumatol.* **2006**, *20*, 983 – 1002.
[20] N.-G. Li, Z.-H. Shi, Y.-P. Tang, Z.-J. Wang, S.-L. Song, L.-H. Qian, D.-W. Qian, J.-A. Duan, *Curr. Med. Chem.* **2011**, *18*, 977 – 1001.
[21] A. D. Rowan, G. J. Litherland, W. Hui, J. M. Milner, *Expert Opin. Ther. Targets* **2008**, *12*, 1 – 18.
[22] R. Renkiewicz, L. Qiu, C. Lesch, X. Sun, R. Devalaraja, T. Cody, E. Kaldjian, H. Welgus, V. Baragi, *Arthritis Rheum.* **2003**, *48*, 1742 – 1749.
[23] I. M. Clark, A. E. Parker, *Expert Opin. Ther. Targets* **2003**, *7*, 19 – 34.
[24] C. Gege, B. Bao, H. Bluhm, J. Boer, B. M. Gallagher, B. Korniski, T. S. Powers, C. Steeneck, A. G. Taveras, V. M. Baragi, *J. Med. Chem.* **2012**, *55*, 709 – 716.
[25] A. R. Johnson, A. G. Pavlovsky, D. F. Ortwine, F. Prior, C.-F. Man, D. A. Bornemeier, C. A. Banotai, W. T. Mueller, P. McConnell, C. Yan, V. Baragi, C. Lesch, W. Howard Roark, M. Wilson, K. Datta, R. Guzman, H.-K. Han, R. D. Dyer, *J. Biol. Chem.* **2007**, *282*, 27781 – 27791.
[26] H. Nara, K. Sato, T. Naito, H. Mototani, H. Oki, Y. Yamamoto, H. Kuno, T. Santou, N. Kanzaki, J. Terauchi, O. Uchikawa, M. Kori, *J. Med. Chem.* **2014**, *57*, 8886 – 8902.
[27] T. Fischer, R. Riedl, *Int. J. Mol. Sci.* **2016**, *17*, 314.
[28] J. Lanz, R. Riedl, *ChemMedChem* **2015**, *10*, 451 – 454.
[29] H. Nara, K. Sato, A. Kaieda, H. Oki, H. Kuno, T. Santou, N. Kanzaki, J. Terauchi, O. Uchikawa, M. Kori, *Bioorg. Med. Chem.* **2016**, *24*, 6149.
[30] T. Fischer, R. Riedl, *ChemMedChem* **2013**, *8*, 1457 – 1461.
[31] B. K. Park, N. R. Kitteringham, P. M. O'Neill, *Annu. Rev. Pharmacol. Toxicol.* **2001**, *41*, 443 – 470.
[32] B. K. Park, N. R. Kitteringham, *Drug Metab. Rev.* **1994**, *26*, 605 – 643.
[33] J. W. Clader, *J. Med. Chem.* **2004**, *47*, 1 – 9.

[34] M. J. Shaughnessy, A. Harsanyi, J. Li, T. Bright, C. D. Murphy, G. Sandford, *ChemMedChem* **2014**, *9*, 733 – 736.
[35] S. Ye, B. Loll, A. A. Berger, U. Mülow, C. Alings, M. C. Wahl, B. Koksch, *Chem. Sci.* **2015**, *6*, 5246 – 5254.
[36] J. A. Olsen, D. W. Banner, P. Seiler, U. Obst Sander, A. D'Arcy, M. Stihle, K. Müller, F. Diederich, *Angew. Chem. Int. Ed.* **2003**, *42*, 2507 – 2511; *Angew. Chem.* **2003**, *115*, 2611 – 2615.

Received: November 28, 2016
Published online on January 12, 2017

